

UMA ABORDAGEM PARA ESTIMAR A TAXA DE FORMAÇÃO DE DEPÓSITO
ORGÂNICO EM UMA HASTE E SELEÇÃO DE MÉTODOS PARA PREVENÇÃO DE
DEPÓSITO

AN APPROACH TO ESTIMATING THE RATE OF ORGANIC DEPOSIT FORMATION IN A
HOLLOW ROD STRING AND SELECTION OF METHODS FOR DEPOSIT PREVENTION

СПОСОБ ОЦЕНКИ ИНТЕНСИВНОСТИ ОБРАЗОВАНИЯ ОРГАНИЧЕСКИХ
ОТЛОЖЕНИЙ В КОЛОННЕ ПОЛЫХ ШТАНГ И ПОДБОР МЕТОДОВ БОРЬБЫ С НИМИ

KRIVOSHCHEKOV, Sergey Nikolaevich^{1*}; VYATKIN, Kirill Andreevich²; KOCHNEV,
Aleksandr Aleksandrovich^{3,4}; KOZLOV, Anton Vadimovich⁵

^{1,2,3,5} Perm National Research Polytechnic University, Mining and Oil Faculty, Perm, Russian Federation

⁴ LUKOIL-Engineering PermNIPIneft LLC, Department of Geological and Hydrodynamic Modeling, Perm,
Russian Federation

* Corresponding author
e-mail: krivoshchekov@gmail.com

Received 05 November 2020; received in revised form 28 December 2020; accepted 20 February 2021

RESUMO

Introdução. Atualmente, falta uma metodologia que possa permitir determinações altamente precisas das taxas de formações de depósito de asfalteno (AD) em caso de operação dupla de dois reservatórios de petróleo por meio de um único poço multi-zona produtor de petróleo usando hastes oca de pequeno diâmetro parte do equipamento de bombeamento de fundo de poço. Essa metodologia visa minimizar os custos das empresas de petróleo e gás com a manutenção de tais poços de petróleo e prevenir o seu fracasso. **Objetivos.** Criação de uma metodologia voltada para estimativas quantitativas precisas das taxas de formação de depósitos orgânicos na parte interna das colunas de hastes oca. **Métodos.** Cálculos de distribuições de temperatura ao longo da superfície interna da coluna de haste oca; apresentações gráficas dos dados calculados; testes de laboratório usando uma unidade Cold Finger para as seções selecionadas das cordas da haste oca e as apresentações gráficas dos resultados. **Resultados e discussão.** O algoritmo sugerido foi testado em campo em um poço produtor de petróleo multi-zona alvo do campo de petróleo Pavlovka em Perm Krai da Federação Russa. Usando o algoritmo sugerido, uma variação nas taxas de formação de depósito orgânico ao longo do comprimento da coluna de haste oca foi avaliada e a profundidade da taxa máxima de formação de depósito foi determinada. Para evitar os depósitos em questão ao longo da coluna de haste oca em um poço produtor de petróleo alvo do campo de petróleo de Pavlovka, testes de laboratório foram conduzidos para determinar a eficiência do emprego da tecnologia química, ou seja, o uso de inibidores de AD, bem como uma tecnologia para a remoção dos depósitos formados usando solventes AD. **Conclusões.** O algoritmo proposto é mais preciso e requer menos tempo e dinheiro em comparação com os algoritmos existentes. Permite uma avaliação mais eficaz da profundidade de formação dos depósitos orgânicos e da intensidade nestas marcas. Ao avaliar os resultados dos estudos laboratoriais, pode-se notar que o uso das tecnologias consideradas para eliminar depósitos orgânicos é altamente eficaz e pode ser utilizado para este fim.

Palavras-chave: depósito de asfalteno, operação dupla, poços com várias zonas, temperatura, inibidor.

ABSTRACT

Background. There is currently a lack of a methodology that can enable highly-precise determinations of rates of asphaltene deposit (AD) formations in case of dual operation of two oil reservoirs via a single multi-zone oil-producing well using small-bore hollow rods as part of downhole pumping equipment. This methodology aims to minimize the costs of oil and gas companies for servicing such oil wells and preventing their failure. **Aims.** Creating a methodology aimed at accurate quantitative estimations of the organic deposit formation rates at the inner part of the hollow rod strings. **Methods.** Calculations of temperature distributions along the hollow rod

string inner surface; graphic presentations of the calculated data; laboratory tests using a Cold Finger unit for the selected sections of the hollow rod strings and the graphic presentations of the results. **Results and Discussion.** The suggested algorithm was field-tested at a target multi-zone oil-producing well of Pavlovka oil field in Perm Krai of the Russian Federation. Using the suggested algorithm, a variation in organic deposit formation rates along the hollow rod string length was evaluated, and the depth of the maximum deposit formation rate was determined. To prevent the deposits in question along the hollow rod string at a target oil-producing well of Pavlovka oil field, laboratory tests were conducted to determine the efficiency of employing the chemical technology, i.e., the use of AD inhibitors, as well as a technology for the removal of the formed deposits using AD solvents. **Conclusions.** The proposed algorithm is more accurate and requires less time and money compared to existing algorithms. It enables the most effective evaluation of the formation depth of the organic deposits and the intensity at these marks. When evaluating the laboratory studies results, it can be noted that the use of the considered technologies to eliminate organic deposits is highly effective and can be used for this purpose.

Keywords: asphaltene deposit, dual operation, multi-zone wells, temperature, inhibitor.

ABSTRACT

Актуальность: Актуальность исследования обусловлена отсутствием методики позволяющей с высокой точностью определить характер и степень изменения интенсивности образования асфальтосмолопарафиновых отложений при одновременно – раздельной эксплуатации двух нефтяных пластов единой транзитной нефтедобывающей скважиной с применением в составе глубинно-насосного оборудования полых штанг с малым внутренним диаметром. Применение данной методики направлено на минимизацию затрат нефтегазовых компаний на обслуживание данных нефтедобывающих скважин и предотвращение их отказа. **Цель:** создать методику, позволяющую осуществлять точно количественное определение интенсивности образования органических отложений на внутренней поверхности полых штанг. **Методы:** расчет распределения температуры внутренней поверхности колонны полых штанг; графическое представление расчетных данных; проведения лабораторных исследований на установке «Холодного стержня» в выбранных, по итогу анализа графических данных сечениях колонны полых штанг, и графическое представление результатов. **Результаты и Обсуждение:** Предложенный алгоритм апробирован на целевой транзитной нефтедобывающей скважине Павловского нефтяного месторождения Пермского края Российской Федерации. В результате применения предложенного алгоритма получено изменение интенсивности образования органических отложений по длине колонны полых штанг, определена глубина наибольшей интенсивности образования отложений. С целью борьбы с рассматриваемыми отложениями в колонне полых штанг целевой нефтедобывающей скважины Павловского нефтяного месторождения проведены лабораторные исследования по определению эффективности применения технологии химизации–применение ингибиторов асфальтосмолопарафиновых отложений, а также технологии удаления сформировавшихся отложений растворителями асфальтосмолопарафиновых отложений. **Заключение:** Предложенный алгоритм обладает большей точностью и требует меньших временных и денежных затрат в сравнении с существующими алгоритмами. Используя данный алгоритм становится возможным наиболее эффективно оценивать глубины образования органических отложений и интенсивность на данных отметках. Оценивая результаты лабораторных исследований можно отметить что применение рассматриваемых технологий борьбы с органическими отложениями высокоэффективно и может использоваться для данной цели.

Keywords: асфальтеносмолопарафиновые отложения, одновременно-раздельная эксплуатация, транзитные скважины, температура, ингибитор.

1. INTRODUCTION:

At present, a crucial task for oil production enterprises is to improve the profitability of oil-producing wells operation in the context of decreasing hydrocarbon production rates and increased proportion of difficult oil fields with production zones featuring low permeability, low net oil pay values, and complicated pore volume structure, which raise the question of employing the technologies for increasing the technical and

economic efficiency of the development of oil fields (Bahgizin *et al.*, 2019; Shaislamov *et al.*, 2007; Putilov, I. *et al.*, 2020).

Among such technologies is dual operation (DO) of multi-zone wells. This technology is used for the following purposes:

- Operation of multi-zone formations where productive reservoirs may be separated into numerous interlayers.
- Reduction of capital investment and

operating costs related to oil field drilling and operation.

- Enabling of accounting of recovered products from each reservoir along with a working agent injected into it.
- Operating the formations featuring multiple productive reservoirs exhibiting stark difference regarding their geological and geophysical parameters as well as the chemical composition of recovered products (Ivanov *et al.*, 2013; Garifov *et al.*, 2013)

Field experience with operating two and more production facilities of a single multi-zone oil-producing well demonstrates the high efficiency of this technology. On average, capital investment and operating costs are reduced by 30 % as compared with the costs related to oil field drilling and operation utilizing individual networks at each oil reservoir (Nurgaliev and Habibullin, 2016). The use of dual operation technology enables increasing the density of well networks without increasing the drilling depth. The increased operational efficiency results in the increased capacity of oil-producing wells. Therefore, the DO technology enables a significant reduction in oil production costs (Ivanovskij, 2010; Josset *et al.*, 2015; Nurgaliev and Habibullin, 2015).

At present, multiple design solutions are available for dual operation equipment. Examples of existing DO units are detailed in papers (Shrajbman *et al.*, 2008; Pepeljaev and Krivonosov 2008, 2009; Volodin *et al.*, 2008). Upon analyzing the specified papers, it can be concluded that hollow pumping rods are often used as part of equipment employed for the dual operation of two oil reservoirs. Among the practical advantages of employing hollow rods are the following (Latypov, 2012; Hisamov *et al.*, 2009; Krjakushin *et al.*, 2009).

- Capability of monitoring bottom-hole pressure across the upper development facility by marking the dynamical level value.
- Capability of taking separate oil flow rate measurements and separate samples at each development facility.
- Capability of process washing of downhole pumping equipment operating both in the upper and lower productive intervals.
- Increasing the rate of fluid lifting along the wellbore.

Among disadvantages of employing hollow rods, an increased withdrawal of sand

from the bottom hole can be considered along with the fact that selection and calculation of hollow rods can be difficult due to design complexity and presence of concentric pressure as well as reservoir fluid impact upon both the inner and outer rod walls (Dubinov, and Ivanovskij, 2016)

The use of hollow rods enables separate operation of two oil reservoirs; however, in this scenario, lifting of products recovered from one of them is performed along a string with a small hydraulically equivalent diameter. Hollow rods with an inner diameter of 9.52 to 18.0 mm are employed at Russian oil fields. Lifting of fluid along a small-bore string is often hindered by organic deposits, which results in the built-up of additional hydraulic resistance. Engineers implementing the DO technology employing hollow rods must anticipate the possibility of organic deposit formation in a hollow rod string and select appropriate technologies for taking care of possible hindrances to prevent premature failure of downhole pumping equipment.

At present, various methods are available to forecast the possibility of organic deposit formation in an oil-producing well. These methods can be divided into three groups.

The first group of methods presented in the works of Turbakov *et al.* (2009), Kishhenko *et al.* (2018), Erofeev *et al.* (2010), and Osipov *et al.* (2016) involves solving two mathematical equations in sequence.

Examples of these equations are presented in Equations 1 and 2. The first expression describes the change in the temperature of the inner surface of the tubing. The second expression is an empirical formula aimed at determining the paraffin saturation temperature of degassed oil.

$$t_{ct} = t_{pl} - (H_{ckb} - H) \cdot \frac{0,034 + 0,725 \cdot \omega}{10^{Q/(1728 \cdot \rho_f \cdot d^{2,67})}} \quad (Eq.1)$$

$$t_{hac} = 70,5 \cdot e^{-\frac{3,686}{\Pi}} \quad (Eq.2)$$

where t_{ct} is the hollow rod inner surface temperature, $^{\circ}\text{C}$; t_{pl} is formation temperature (fluid temperature in the downhole) $^{\circ}\text{C}$; ω is geothermic gradient, $^{\circ}\text{C}/\text{m}$; H_{ckb} is the well depth, m ; H is the depth from the well mouth, m ; Q is the well mass discharge with flow rate, t/day ; ρ_f is the fluid density, kg/m^3 ; d is inner diameter of the liquid transporting pipe, m ; Π is the mass fraction of asphaltenes in oil, %.

The first equation is a function of temperature distribution along the inner surface of a rod through which lifting of fluid is performed inside the well. The second equation is a function of the temperature of oil saturation with paraffin dependent on various physical parameters; this function can be evaluated based on various empirical dependencies. In these dependencies, the following factors affect the temperature of oil saturation with paraffin: pressure and gas content distribution along the wellbore, the mass fraction of asphaltenes, resins, and paraffin in the produced fluid, as well as oil saturation temperature under surface conditions. Among the disadvantages of this group of methods is that it is only possible to evaluate the depth at which organic deposit formation begins and the introduction of significant errors related to the determination of the temperature of oil saturation with paraffin. This error is composed of three constituents: continuous change of physical and chemical properties of the recovered fluid in the production process, variation in pressure distribution along the wellbore as well as consequent variation in gas content, and availability of various methods for estimating the temperature of degassed oil saturation with paraffin. Among them are visual, refractometric, rheological, volumetric, gravimetric, photometric methods, nuclear magnetic resonance methods, and differential scanning calorimetry.

The second group of methods is presented in the works of Misnik and Galikeev (2011) and (Korobov and Rogachev, 2015). This method is based on the study of asphaltene (A), and resinous (R) compounds impact on the paraffin formation process and, in particular, on paraffin crystallization temperature. This method describes a linear statistical relationship between A/R ratio and field data representing depths of well clean-up and organic deposits. Among disadvantages of this method is a continuous variation of the A/R ratio in recovered products, the presence of numerous deviations from the suggested linear law, as well as the need to conduct multiple laboratory tests and obtain statistical data to determine the linear law of interest for each of the surveyed oil fields.

The third group of methods features Robinson and Peng equations of state (Robinson and Peng, 1976) and is presented in the work of Falovskij *et al.* (2011), Farayola *et al.* (2010), and Dalirsefat and Feyzi (2007). This method is based on laboratory tests used to determine critical parameters of each component in a

hydrocarbon mixture. Upon discovering the critical parameters, it is possible to determine Pressure Volume Temperature (PVT) ratios for the hydrocarbon mixture in question. This method has some disadvantages, i.e., the need to employ expensive equipment, reliance on sophisticated mathematical techniques, and excessive time-consuming laboratory researches and subsequent mathematical calculations.

In light of all of the above, it becomes evident that the problem of lacking a precise method for determining the depth at which organic deposit formation begins in oil-producing well and in particular in hollow rod strings needs to be addressed with the vital task of discovering ways to assess the rate of organic deposit formation. High-accuracy forecasting of organic deposit formation rate is crucial when operating small-bore downhole pumping equipment.

2. MATERIALS AND METHODS

The target facility for determining the pattern of the hollow rod inner surface temperature variation along its length, a multi-zone oil-producing well of Pavlovka oil field in Perm Krai of the Russian Federation, was selected. To estimate the hollow rod inner surface temperature under the method described in the Methods chapter, the values presented in Table 1 were required. These values included both the physical and chemical properties of the recovered product and the geothermic properties of the well. All considered values were determined by the technological documents or the previous laboratory surveys of the studied target facility. However, the geothermal gradient (ω) was calculated under Equation 3.

$$\omega = \frac{t_{\text{п.л}} - t_{\text{H.C.}}}{D_{\text{п.л}} - D_{\text{H.C.}}} \cdot 100\% \quad (\text{Eq.3})$$

where $t_{\text{H.C.}}$ is reference datum temperature $^{\circ}\text{C}$; $D_{\text{п.л}}$ was base formation top depth, m; $D_{\text{H.C.}}$ was reference datum depth, m.

The given well operates two oil reservoirs. The upper productive interval was TI-Bb interval. The fluids recovered from the reservoir were pumped inside the pumping and compressor pipes (PCP). The lower productive interval was T interval. The fluids recovered from this reservoir

were pumped through the hollow rod string. The downhole pumping equipment installed in the given well was used to separate product from two oil reservoirs.

Table 1. Input data for the hollow rod inner surface temperature distribution calculation

Value	Size	Reservoir	
		T	TI-Bb
$t_{\text{пл}}$	°C	25	24
$D_{\text{пл}}$	m	1479	1470
D_{HACOC}	m	1509	1400
β_{B}	%	8.4	7.1
D_{dyn}	m	-	694
ρ_{f}	kg/m ³	870	834
q	m ³ /day	4.9	13.9
$t_{\text{H.C.}}$	°C	7	
ω	°C/m	0.013	
$d_{\text{ЭК1}}$	mm	146	
$d_{\text{ЭК2}}$	mm	132	
$d_{\text{Ш1}}$	mm	38	
$d_{\text{Ш2}}$	mm	19	
d_{HKT1}	mm	73	
d_{HKT2}	mm	62	
d_{CKB}	mm	216	
λ_{HKT}	W/(m · °C)	64	
$\lambda_{\text{Цемента}}$	W/(m · °C)	1.51	
λ_{H}	W/(m · °C)	0.1325	
λ_{B}	W/(m · °C)	0.593	
$R_{\text{гр}}$	m · °C/W	120	
c_{B}	J/kg · °C	4182	
c_{H}	J/kg · °C	2100	

where D_{HACOC} was pump suspension depth, m; β_{B} was fluid water cut, %; D_{dyn} was dynamical level depth, m; d_{CKB} was the well diameter, mm; $d_{\text{ЭК1}}$ was the outer diameter of the production string, mm; $d_{\text{Ш1}}$ was the outer diameter of the hollow rod, mm; d_{HKT1} was the outer diameter of the pumping and compressor pipe, mm; $d_{\text{ЭК2}}$ was the inner diameter of the production string, mm; $d_{\text{Ш2}}$ was the inner diameter of the hollow rod, mm; d_{HKT2} was the inner diameter of the pumping and compressor pipe, mm; λ_{HKT} was the heat conductivity coefficient of the pump-compressor pipe, W/(m · °C); $\lambda_{\text{Цемента}}$ was cement stone heat conductivity coefficient, W/(m · °C); λ_{B} was water heat conductivity coefficient, W/(m · °C); λ_{H} was oil heat conductivity coefficient, W/(m · °C); $R_{\text{гр}}$ was the thermal resistance of the rock surrounding the well, m · °C/W; c_{B} was water heat

capacity, J/kg · °C; c_{H} was oil heat capacity, J/kg · °C.

Forecasting asphalt deposits (AD) formation in hollow rods of a target facility required plotting a chart representing surface temperature distribution along the length of hollow rod inner wall. The following initial data were required for this calculation:

- Geometric characteristics and thermal conductivity of the material of cement stone (CS), production string (PS), pumping and compressor pipes (PCP), and hollow rods.
- Well production rate.
- Depth and temperature of the reference datum in the given region.
- Top and bottom temperature and elevations of the operated oil reservoirs.
- Pump-setting depth.
- Thermal conductivity of geological material around the well.
- Dynamical level value of the given well.
- Physical and chemical properties of liquid fluids (density, dynamic viscosity, water cut of recovered products, and thermal conductivity).
- Associated petroleum gas composition.

The pattern of inner wall surface temperature variation along hollow rod length was determined based on expressions presented in (Korobov and Mordvinov, 2013; Gorshkov, 2014; Krajnov *et al.*, 2010; Malashkina, 2015). First, it was required to calculate the total thermal resistance as per Equation 4 for fluids recovered from both productive reservoirs:

$$K = \frac{1}{\frac{1}{\alpha} + R} \quad (\text{Eq.4})$$

where α was the internal pipe fluid heat transfer coefficient, W/(m² · °C); R was the thermal resistance of the media surrounding the well, m² · °C/W; K_T was the coefficient of heat condition from the fluid to the environment, W/(m² · °C).

Coefficient α was calculated based on the criteria dependent function for laminar flow presented in Equation 5:

$$\alpha = 4 \cdot \frac{\lambda_t}{d} \quad (\text{Eq.5})$$

where λ_t was pipe material heat conductivity coefficient, W/(m · °C).

Coefficient R could be calculated based on Equation 6:

$$R = \sum \frac{h_i}{\lambda_i} \quad (\text{Eq.6})$$

where λ_i was insulating material heat conductivity coefficient, $\text{W} / (\text{m} \cdot ^\circ\text{C})$; h_i was insulation layer thickness, m

However, coefficient R could not be applied to the entire well depth because different components determine it. For this reason, calculations were made for three different thermal resistance modes and their corresponding sections: from bottom-hole to pump-setting depth (R_1), from pump-setting depth to dynamical level (R_2), from dynamical level to well-head (R_3). Under all three modes, thermal resistance was an aggregate of various combinations of resistance values corresponding to hollow rod body, the fluid moving inside pumping and compressor pipes (PCP) string, casing string PCP wall, cement stone, and geological material around the well.

By applying Equations 5 and 6 to expression Eq. 7, the following was obtained:

$$K_T = \frac{1}{\frac{d}{4 \cdot \lambda_t} + \sum \frac{h_i}{\lambda_i}} \quad (\text{Eq.7})$$

Coefficient K was calculated based on the assumption of complete alignment of all well components. Because coefficient R varied along with the well depth, coefficient K varied within a similar range.

To determine the pattern of temperature variation along the wellbore, Equation 8 was written down. Its left-hand member was representing the quantity of heat given up by liquid in the elementary area dL upon lifting the recovered products by PCP or hollow rod with the lateral area amounting to $\pi \cdot D \cdot dL$. The right-hand member of this expression represented the decrease of fluid temperature upon its lifting.

$$K_T \cdot [t_{\text{cr}} - (t_{\text{nl}} - \omega \cdot L)] \cdot \pi \cdot d \cdot dL = c_f \cdot \omega \cdot \rho_f \cdot u \cdot F_{\text{tp}} \cdot dt_f \quad (\text{Eq.8})$$

where L was the vertical distance from the bottom-hole to the studied elementary pipe section, m ; dL was elementary pipe section, m ; c_f was water-in-oil emulsion heat capacity $\text{J} / \text{kg} \cdot ^\circ\text{C}$; u was the average fluid flow rate, m/sec ; F_{tp} was a clear opening area, m^2 ; dt_f was a fluid temperature change in the elementary section, $^\circ\text{C}$.

To perform the integration of Equation 8, it

was required to use the equation of integration constant (C_1), which was determined based on initial conditions with $h = 0$ и $t_{\text{cr}} = t_{\text{nl}}$ obtained from Equation 9:

$$C_1 = \frac{c_f \cdot \omega \cdot \rho_f \cdot q}{K_T \cdot \pi \cdot d} \quad (\text{Eq.9})$$

where q was volumetric fluid flow, m^3 / day .

In Eq. 8, the product of the average fluid flow rate (u) and clear pipe area (F_{tp}) corresponded to the volumetric flow rate value presented in Equation 10:

$$u \cdot F_{\text{tp}} = q \quad (\text{Eq.10})$$

A solution to Eq. 8, taking into account Eq. 10, was found via Eqs. 11 or 12:

$$t_{\text{cr}} = t_{\text{nl}} - \omega \cdot L + \frac{c_f \cdot \omega \cdot \rho_f \cdot q}{K_T \cdot \pi \cdot d} - C_1 \cdot e^{\frac{K_T \pi \cdot d \cdot L}{c_f \rho_f q}} \quad (\text{Eq.11})$$

$$t_{\text{cr}} = t_{\text{nl}} - \omega \cdot L + \frac{c_f \cdot \omega \cdot \rho_f \cdot q}{K_T \cdot \pi \cdot d} \cdot \left(1 - e^{\frac{K_T \pi \cdot d \cdot L}{c_f \rho_f q}} \right) \quad (\text{Eq.12})$$

Upon calculating inner temperature distribution across hollow rod surface along the well length, a chart was plotted based on Eq. 11. The created chart was required to select several sections with characteristic temperatures (maximum, minimum, closest to the initial paraffin crystallization temperature (IPCT)) and intermediate temperature values. The obtained temperature values would be subsequently used in laboratory tests for determining the rate of AD formation on the Cold Finger unit. To improve the accuracy of tests conducted on this unit, 4 unconnected Cold Fingers were used simultaneously. Because the Cold Finger unit was a "reverse pipeline", the temperature of the refrigerant fluid used for cooling the inner surface of Cold Fingers was taken as equal to the temperature of the hollow rod inner surface, which was calculated based on Equation 11. The assessed oil sample mixing speed was taken based on the calculated recovered products flow rate along the internal surface of hollow rods. Based on the obtained laboratory test results, the rate of AD formation was assessed using Equation 13:

$$I = \frac{m_{\text{AD}}}{m_{\text{oil}}} \cdot 100 \quad (\text{Eq.13})$$

where I was AD formation intensiveness, %; m_{AD} was the mass of adhered AD equal to the difference of the Cold Finger masses before and after survey, g; m_{oil} was AD mass of the studied oil sample, g.

The effectiveness estimation of applying inhibitor reagents was made according to Equation 14:

$$K_{ing} = \frac{I_2 - I_1}{I_2} \cdot 100\% \quad (\text{Eq.14})$$

where K_{ing} is specific inhibition capacity, %; I_1 is AD formation intensiveness after AD inhibitor application, %; I_2 is AD formation intensiveness before AD inhibitor application, %.

The effectiveness estimation of the hydrocarbon solvents was made based on Equation 15.

$$K_s = \frac{m_{AD2} - m_{AD1}}{m_{AD2}} \cdot 100\% \quad (\text{Eq.15})$$

3. RESULTS AND DISCUSSION

3.1. Calculation of the technological parameters of the target multi-zone oil-producing well operating two oil reservoirs

The temperature distribution along the well depth was carried out with the algorithm presented in the Methods chapter. The preparatory stage of the calculation is the determination of such parameters as thermal resistance of the media surrounding the well (R), coefficient of heat conductivity from the fluid to the environment (K_T), water-in-oil emulsion heat conductivity coefficient (λ_f), water-in-oil emulsion heat capacity (c_f) and inner pipe surface fluid heat transfer coefficient, (α). Calculation R , K_T , α is carried out under Eqs. 3,1,2 respectively. The water-in-oil emulsion heat capacity values (c_f) are used by Eq. 16. The water-in-oil emulsion heat conductivity values are found in Eq. 17.

$$c_f = c_H \cdot (1 - \beta_B) + c_B \cdot \beta_B \quad (\text{Eq.16})$$

$$\lambda_f = \lambda_H \cdot \left[\frac{2 \cdot \lambda_H + \lambda_B - 2 \cdot \beta_B \cdot (\lambda_H - \lambda_B)}{2 \cdot \lambda_H + \lambda_B + 2 \cdot \beta_B \cdot (\lambda_H - \lambda_B)} \right] \quad (\text{Eq.17})$$

These parameters need to be determined for the three intervals the producing well was conventionally divided into. The first interval is the distance from the depth of reservoir T to the

pump suspension depth (R_1, K_{T1}), the second is the distance from the pump suspension depth to the dynamical level mark (R_2, K_{T2}), and third is the distance from the dynamical level mark to the oil-producing well mouth (R_3, K_{T3}). The parameters calculated for the given producing well are presented in Table 2.

Based on Equation 11, the temperature graph of the inner surface of the pumping and compressor pipes used for pumping product from Ti-Bb reservoir and the temperature graph of the inner surface of the hollow rod body string transporting the product from T reservoir have been formed and presented in Figure 1.

Analysing Figure 1, we may conclude that the temperature of the inner surface of the hollow rods changes more intensively compared to the inner surface of the pumping and compressor pipes (PCP). This is explained by the fact that the fluid recovered from reservoir T features two additional thermal resistance values (resistance of the liquid layer and resistance of the hollow rod body). For this reason, the fluid loses temperature faster as it approaches the well mouth. The reason for changing the temperature distribution pattern above the dynamic level (D_{dyn}) is the change of the fluid contained in the annulus (thermal resistance of the gas mix increases the same oil parameter several-fold).

3.2. The result of determining possibilities of the organic deposit formations according to the methods described in paragraph 1

The solution of the equations describing the temperature of the string and the temperature of oil saturation with paraffin, which are the first group of methodologies, is shown in Figure 2. The second group of methodologies does not have a graphical solution, since it is based on the analysis of the existing graphs of the dependence of the formation depth of the organic deposits on the ratio of asphaltene and resinous phase. According to the results of this analysis, for the fluid under consideration, the ratio of the mass content of asphaltenes to resins (A/R) is 0.21, and the depth of the onset of sediment formation is 600 m. Application of the third group of methodologies is not possible due to the need for

high-precision and expensive equipment, which is its main disadvantage.

After analyzing this graph and the results given for the second group of methods, we can say that these methods are inaccurate, do not take into account many factors and are based on empirical dependencies, not on laboratory studies, so we cannot recommend them for use.

3.3. Determination of the intensiveness of AD formation in laboratory conditions

The laboratory studies of AD formation intensiveness were carried out with the CF-4 cold finger unit presented in Figure 3.



Figure 3. The Cold Finger laboratory unit CF-4

Based on the analysis of Fig. 1 for the laboratory studies of the AD formation intensiveness, 5 temperatures were selected to match the estimated temperatures of the inner surface of the hollow rod within the given intervals of the well depth. In each of the intervals, the studies were carried out at the sample mixing rate of 300 rpm for 25 minutes, which equals the time of fluid elevation through the studied intervals. The study was carried out on 4 samples simultaneously and under the same conditions to minimize the possible error of the survey results. The AD formation intensiveness was assessed based on Equation 13. Figure 4 presents the examples of Cold Fingers before the survey and after its completion.

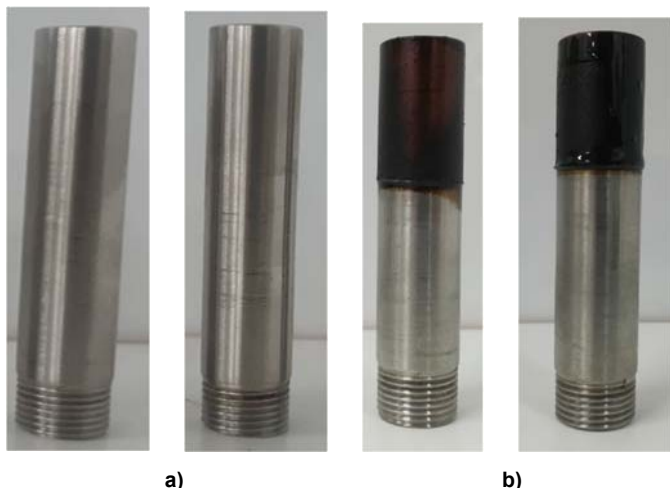


Figure 4. Cold Finger picture example: a) before the survey; b) after the survey

Table 3 shows the results of the survey of the AD formation intensiveness within the studied intervals.

Table 3. AD formation intensiveness in the studied intervals

t_{III} , °C	I , %
24.29	0
22.21	0.33
16.47	0.30
11.35	0.27
7.36	0.31

where t_{III} is Hollow rod inner surface temperature, °C.

Analyzing these data, we may conclude that the intensiveness of AD formation on the inner surface of the hollow rod changes throughout the rod length. The most intensive AD formation process was found at the temperature of 22.21 degrees, which corresponds to the depth of 1079 meters from the well mouth. This peak of AD formation intensiveness is associated with the drop of recovered fluid temperature below the paraffin appearance temperature (IPCT), and then below the mass paraffin phase appearance temperature (MPAT). As the temperature further drops to 16.47 °C, and then to 11.35 °C at a depth of 779 m and 379 m, respectively, the AD formation intensiveness correspondingly reduces. This fact may be explained by the active precipitation of AD previously, at a depth of 1079 m, and the absence of sufficient temperature gradient between the fluid and the hollow rod inner surface. At the temperature of 7.36 °C, the second peak of AD formation intensiveness is observed in the well mouth. This peak may be

associated with the intensive growth of the temperature gradient between the hollow rod inner surface and the recovered fluid.

The collected results of the laboratory survey of the changes in the intensiveness of the AD formation in the hollow rod string are depicted in the temperature graph of the inner surface of the hollow rod string and the inner surface of the PCP string and presented in Figure 4.

In Figure 4, it can be seen two epicenters of AD formation within the studied oil-producing well. During operation, the greatest share of the organic deposits forms at a depth of 800-1100 meters, thereby facilitating the emergence of additional hydraulic resistances. Generally, as a result of the simulation of oil elevation through the hollow rod string, 0.76 g of asphaltene deposits for the studied 63.677 g of oil was found.

3.4. Determination of technological efficiency of the counter-AD technologies used in the hollow rod strings

At the present moment, there are many methods of AD appearance prevention. The most economically feasible and efficient individual counter-AD technology shall be selected in the diversity of recovered fluids and recovery conditions at every target facility (Caeiro *et al.* 2015). There is a known classification of counter-AD formation methods that divides all methods into two groups: AD formation prevention methods and methods of combating the developed deposits. Different deposit combat measures shall be applied depending on the physical, chemical, and rheological properties of the recovered fluids, their composition, temperature, and recovery conditions. These methods may be classified into thermal, chemical, physical, and mechanical. The thermal methods are based on heating the oil above the IPCT temperature followed by the dissolution of the wax component of the fluid, preventing its recovery from the fluid volume (Putilov, *et al.*, 2020; Revel'-Muroz *et al.*, 2017 Reza and Farzaneh, 2007) The chemical methods assume the application of the reagents preventing the AD formation (inhibitor reagents) or the substances that eliminate the existing deposits (hydrocarbon solvents, detergents) (Robinson and Peng, 1976; Shaislamov, *et al.*, 2007; Shrajbman, *et al.*, 2008). The physical methods require various physical fields (magnetic, acoustic, ultrasound, electric) and mechanic deposit removal methods (Turbakov, *et al.*, 2009; Volodin, *et al.*, 2008). Due to the specificity of a configuration of the

downhole pumping equipment used for dual operation (DO), there are certain restrictions for the applicability of the counter-AD measures.

This way, it was considered two AD removal technologies applicable for this type of oil operation, which are the application of chemicals (inhibitor reagent application) and AD removal using hydrocarbon solvents.

The research of technological efficiency of applying the inhibitor reagents to prevent deposit formation on the inner surface of the hollow rods was carried out with the Cold Finger unit. The research covered three different reagents: FLEK-IP-106, EFRIL-IPO417M grade DP and SNPH-7909. The studies were carried on two concentrations for each of the studied reagents: 200 g/tonne and 400 g/tonne. The intensiveness of AD formation under the use of inhibitor reagents was calculated with Eq. 10. The results of these studies are presented in Fig. 5. Upon the results of the laboratory researches, the specific inhibition capacity of the studied reagents was calculated. This property was determined using Eq. 14. These value calculation results are shown in Table 4. Based on the results shown in Figure 5, and in Table 4, it may be concluded that for the oil recovered from the target oil-producing well of Pavlovka oil field, the most efficient AD inhibitor is EFRIL-IPO417M grade DP. The specific efficiency is 48.1% at the chemical reagent dose of 200 g/tonne.

Table 4. Calculated specific efficiency of the studied reagent application

Considered inhibitor	C (g/tonne)	K _{ing} (%)
FLEK-IP-106	200	7.9
	400	-4.0
EFTIL-IPO417M grade DP	200	48.1
	400	12.1
SNPH-7909	200	36.8
	400	29.5

The technological efficiency of AD solvent washes for removing the formed deposits was also determined with the Cold Finger unit. In the current survey, three different AD solvents were used: EFRIL-270, FLEK R-016, RTS-1. The survey was carried out in the AD samples collected from the reservoir fluid collected from the target oil-producing well by sinking the Cold Finger into the free volume of solvent for 60, 120, and 150 seconds. The solvent efficiency was assessed with Eq. 15. The results of the completed laboratory are shown in Table 5.

Table 4. Results of the solvent capacity studies of the considered AD solvents.

Considered solvent	T_{UCCN} (°C)	K_s (%)
EFRIL-270	60	66.4
	120	71.1
	150	74.1
	60	76.3
FLEK R-016	120	86.2
	150	92.4
	60	79.5
RTS-1	120	85.2
	150	88.5

Analyzing these data, it may be noticed that the most efficient AD solvent for the product recovered from the target oil-producing well is FLEK R-016. The solvent capacity coefficient for the treatment time of 150 s was 92.4%.

4. CONCLUSIONS:

1. A method is proposed for assessing the formation rate of the organic deposits on the inner surfaces of the string and hollow rods in case of a dual operation of two oil reservoirs. This method is based on assessing the temperature distribution of the oil-producing well and conducting laboratory studies.

2. The hollow rod inner surface temperature distribution has been calculated. The laboratory survey was carried out to assess the nature and the AD formation intensiveness change degree on the studied surface based on the calculations.

3. The nature and the degree of AD formation intensiveness change on the studied surface have been analyzed. The analysis of the changes may discover the reason for the AD formation intensiveness changes along the depth length. It requires further studies due to the lack of theoretical materials to describe the phenomenon. Based on the AD formation intensiveness change analysis, it became possible to forecast the AD deposit formation in hollow rods and, particularly, to determine the depth of the most intensive organic deposit formation.

4. A comparison of the proposed method for assessing the formation depth of the organic deposits with existing analogs is given. Based on this comparison, we can conclude that the proposed method has high accuracy and efficiency; and we recommend it for use at

existing oil production facilities to explore limitations of its applicability.

5. The technological applicability of the chemical technology (AD solvent and inhibitor application) has been assessed. According to the laboratory survey results, the application of both deposit removal technologies is technologically efficient with the correctly selected reagent.

5. ACKNOWLEDGMENTS:

This research was funded by the state assignment of the Ministry of Science and Higher Education of the Russian Federation as part of a government assignment, grant number FSNM-2020-0027.

6. REFERENCES:

- Bahgizin, R. N.; Urazakov, K. R.; Usmanov, R. V.; Tugunov, P. M. (2019). Investigation of the thermal regime of a productive reservoir during simultaneous and separate operation of rod and electric center-run pump installations. *Oil Industry*, 4: 80-83. DOI: 10.24887/0028-2448-2019-4-80-83.
- Caeiro, M.H.; Demyanov, V.; Soares, A. (2015). Optimized History Matching with Direct Sequential Image Transforming for Non-Stationary Reservoir, *Mathematical Geosciences*, 47(8): 975-994. DOI: 10.1007/s11004-015-9591-0
- Demyanov, V.; Soltani, S.; Kanevski, M.; Canu, S.; Maignan, M.; Savelieva, E.; Timonin, V.; Pisarenko, V. (2001). Wavelet analysis residual kriging vs. neural network residual kriging, *Stochastic Environmental Research and Risk Assessment*, 15(1): 18-32. DOI: 10.1007/s004770000056
- Dubinov, Ju. S.; Ivanovskij, V. N. (2016). Optimization of the hollow pump rod head design. *Oil and Gas Territory* 3: 66-69.
- Erofeev, A. A.; Turbakov, M. S.; Mordvinov, V. A. (2010). To calculate the temperature distribution of oil saturation with paraffin in the production wells of the Siberian oil field. *Perm Journal of Petroleum and Mining Engineering*, 5: 57-60.
- Falovskij, V. I.; Horoshev, A. S.; Shahov, V. G. (2011). Modern approach to modeling phase transformations of hydrocarbon systems using the Peng-

Robinson equation of state. *Izvestija Samarskogo nauchnogo centra Rossiskoj akademii nauk*, 13(4-1): 120-125.

7. Farayola, K. K.; Adeboye, Y. B.; Adekomaya, O. A.; Olatunde, A. O. (2010). Thermodynamics prediction of wax precipitation using the Patel-Teja equation of state. Paper presented at the Nigeria Annual International Conference and Exhibition, Tinapa - Calabar, Nigeria, 31 July – 7 August. SPE 136966 DOI: 10.2118/136966-MS
8. Garifov, K. M.; Kadyrov, A. H.; Ibragimov, N. G., Fadeev, V. G.; Zabbarov, R. G. (2013). Development of technology for simultaneous and separate reservoir exploitation in JSC Tatneft. *Oil Industry*, 7, 44-47.
9. Gawas, K.; Krishnamurthy, P.; Wei, F; Acosta, E.; Jiang, Y. (2015). Study on Inhibition of High-Molecular-Weight Paraffins for South Eagle Ford Condensate. Paper presented at the SPE Annual Technical Conference and Exhibition, Houston, TX, USA, 28-30 September. Paper SPE 174817. <https://doi.org/10.2118/174817-MS> SPE-174817-MS
10. Glushchenko, V.N.; Shipiguzov, L.M.; Yurpalov, I.A. (2007). Evaluation of the effectiveness of asphaltene-resin-paraffin deposits inhibitors. *Oil Industry*, 5: 84-87.
11. Gorshkov, A. S. (2014). Modeling of non-stationary heat transfer processes in wall structures made of aerated concrete blocks. *Magazine of Civil Engineering*, 8 (52): 38-48. DOI: 10.5862/MCE.52.5
12. Hisamov, P. C.; Evdokimov, A. M.; Sultanov, A. S. (2009). Improvement of the oil Field development system using equipment for simultaneous separate well operation. *OILFIELD ENGINEERING*, 5: 33-39.
13. Struchkov, I. A.; Rogachev, M. K. (2017). Risk of Wax Precipitation in Oil Well. *Natural Resources Research*, 26 (1): 67-73. DOI: 10.1007/s11053-016-9302-7
14. Ivanov, D. V.; Chizhov, A. P. (2013). Simultaneous exploitation of small deposits in the conditions of the Melekessky depression deposits. *Problems of collecting, preparing, and transporting oil and petroleum products*, 4 (94): 5-11.
15. Ivanovskij, V. N. (2010). SSO and intellectualization of wells: yesterday, today, tomorrow. *Oil and Gas Territory*, 3: 28-39.
16. Jalalnezhad, M. J.; Kamali, V. (2016). Development of an intelligent model for wax deposition in oil pipeline. *Journal of Petroleum Exploration and Production Technology*, 6(1): 129–133. DOI 10.1007/s13202-015-0160-3
17. Josset, L.; Demyanov, V.; Elsheikh, A.H.; Lunati, I.. (2015). Accelerating Monte Carlo Markov chains with proxy and error models. *Computers and Geosciences*, 85: 38-48. DOI: 10.1016/j.cageo.2015.07.003
18. Kishhenko, M. A.; Aleksandrov, A. N.; Rogachev, M. K.; Kibirev, E. A. (2018). Modeling of the formation of organic deposits of paraffin type during the operation of wells with electric centrifugal pumps. *Exposition Oil & Gas*, 5 (65): 29-34.
19. Korobov, G. Ju.; Mordvinov, V. A. (2013). Temperature distribution in the production well bore. *Oil Industry*, 4: 57-59.
20. Korobov, G. Ju.; Rogachev, M. K. (2015). Investigation of the influence of asphalt-resinous components in oil on the formation of asphalt-resin-paraffin deposits. *Oil and Gas Business*, 3: 162-173.
21. Krajnov, D. V.; Safin, I. Sh.; Ljubimcev, A. S. (2010). Calculation of additional heat losses through heat-conducting inclusions of enclosing structures (on the example of a window slope node). *Magazine of Civil Engineering*, 6: 17-22.
22. Krjakushin, A. I.; Shljapnikov, Ju. V.; Agafonov, A. A.; Nikishov, V. I. (2009). Results and prospects of implementation of simultaneous-separate operation of reservoirs in one well. *Oil and Gas Territory*, 12: 50-53.
23. Latypov, B. M. (2012). Installation of a rod screw pump for oil production in complicated conditions. *Oil and Gas Business*, 10(1): 13-15.
24. Ljapin, A. Ju.; Astahov, A. V.; Mihaljov, Ju. P. (2017). study of the crystallization temperature of paraffins in oil in order to reduce the formation of asphalt-resin-paraffin de-positions. *Science and technologies: oil and oil products pipeline transportation*, 7(6): 28-35. DOI: 10.28999/2541-9595-2017-7-6-28-35

25. Loskutova, Ju. V.; Judina, N. V. (2006). Evaluation of the effectiveness of asphaltene-resin-paraffin deposits inhibitors. *Bulletin of the Tomsk Polytechnic University. Geo Assets Engineering*, 309 (4): 104-108.

26. Malashkina, V. A. (2015). Features of thermodynamic processes in underground degassing pipelines made of composite materials in coal mines. *Mining informational and analytical bulletin (scientific and technical journal)*, (9): 198-204.

27. Misnik, V. V.; Galikeev, R. M. (2011). Method of forecasting the depth of formation of asphalt-resin-paraffin deposits in wells. *Oil and Gas Business*, (6):345-349.

28. Nurgaliev, A. A.; Habibullin, L. T. (2015). Analysis of the efficiency of SSO in small deposits in the South-East of the Republic of Tatarstan. *Interexpo GEO-Siberia*, 2(3): 169-172.

29. Nurgaliev, A. A.; Habibullin, L. T. (2016). Analysis of the efficiency of simultaneous and separate operation of wells in the fields of the South-East of the Republic of Tatarstan. *Interexpo GEO-Siberia*, 2(3): 230-233.

30. Osipov, A. V.; Galiullin, A. A.; Piskarev, M. A.; Gribennikov, O. A.; (2016). Determination of the depth of the beginning of paraffin crystallization. *Scientific research: from theory to practice*, (3), 205-208. DOI: 10.21661/r-112093

31. Pepeljaev V.V.; Krivonosov Ju.A. (2009). Hollow pump rod. *Patent of the Russian Federation № 2371565*.

32. Pepeljaev V.V.; Krivonosov Ju.A. (2008). Hollow pump rod. *Patent of the Russian Federation № 2398091*.

33. Putilov, I.; Krivoshchekov, S.; Vyatkin, K.; Kochnev A.; Ravelev K. (2020). Methods of predicting the effectiveness of hydrochloric acid treatment using hydrodynamic simulation, *Applied Sciences (Switzerland)*, 10 (14). DOI: 10.3390/app10144828

34. Revel'-Muroz, P. A.; Bahtizin, R. N.; Karimov, R. M.; Mastobaev, B. N. (2017). Joint use of thermal and chemical methods of influence during transportation of high-viscosity and solidifying oils. *SOCAR Proceedings*, 2(2): 49-55.

35. Reza, D.; Farzaneh, F. (2007). A thermodynamic model for wax deposition phenomena. *Fuel*, 86 (10-11): 1402-1408. DOI: 10.1016/j.fuel.2006.11.034

36. Robinson, D.B.; Peng, D.Y. (1976). A New Two-Constant Equation of State Industrial and Engineering Chemistry: Fundamentals. *Industrial & Engineering Chemistry Fundamentals*, 15: 59-64. <http://dx.doi.org/10.1021/i160057a011>

37. Shaislamov, Sh. G.; Antonin, R. A.; Antonin, A. S.; Laptev, V. V. (2007). About simultaneous operation of several layers (interlayers) by one well. *Drilling and Oil*, (10): 21-23.

38. Shrajbman, V. M.; Kolupaev, A. M.; Dolmatov, V. P.; Ponurovsky, A. G. (2008) Method of making a pump rod. *Patent of the Russian Federation № 2342216*.

39. Turbakov, M. S.; Erofeev, A. A.; Lekomcev, A. V. (2009). For determining the depth of the early formation of asphaltenes-operating with sediments in the operation of oil wells. *Geology, geophysics and development of oil and gas fields*, (10): 62-65.

40. Volodin, A. M.; Artes, A. E.; Sorokin, V. A.; Sosenushkin, E. N.; Petrov, N. P.; Tretyukhin, V. V.; Sharapov, K. M. (2008) Method for manufacturing a hollow pump rod for gas and oil wells. *Patent of the Russian Federation № 2384384*.

Table 2. Interim results of the calculation of temperature distribution along with the target oil-producing Pavlovka oil field well. Source: the author

Value	Size	Reservoir					
		T			Tl-Bb		
		Interval					
R	$\text{m}^2 \cdot ^\circ\text{C}/\text{W}$	1	0.41	2	0.33	3	1.36
K_T	$\text{W}/(\text{m}^2 \cdot ^\circ\text{C})$	2.24		2.72	0.71	-	-
c_f	$\text{J}/\text{kg} \cdot ^\circ\text{C}$			2238.6			2217.15
λ_f	$\text{W}/(\text{m} \cdot ^\circ\text{C})$			0.151			0.148
α	$\text{W}/(\text{m}^2 \cdot ^\circ\text{C})$			36.04			27.53

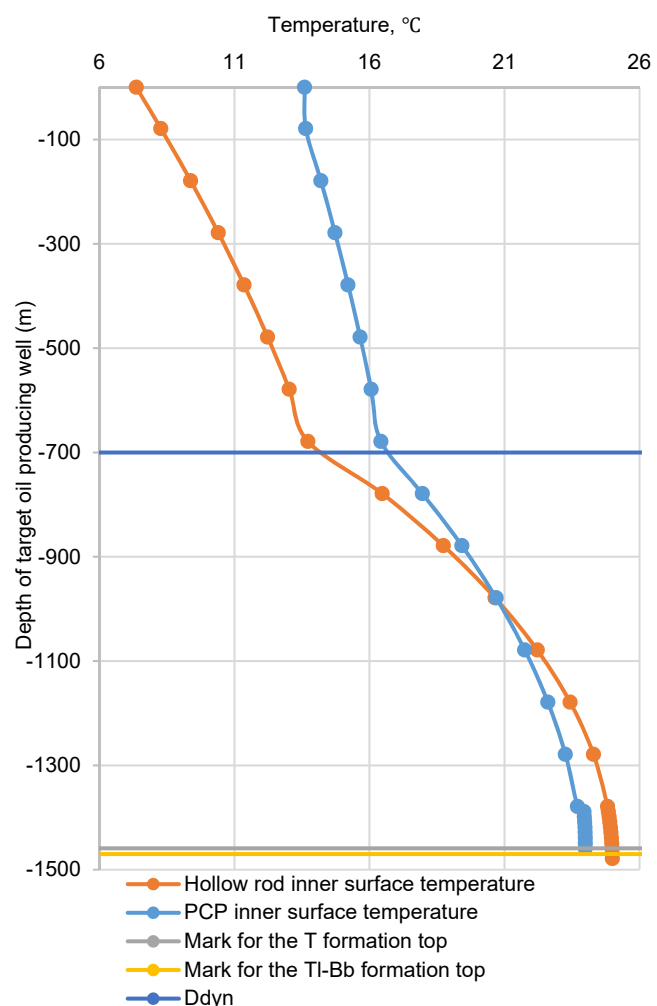


Figure 1. PCP string inner surface temperature graph and the hollow rod string inner surface temperature graph

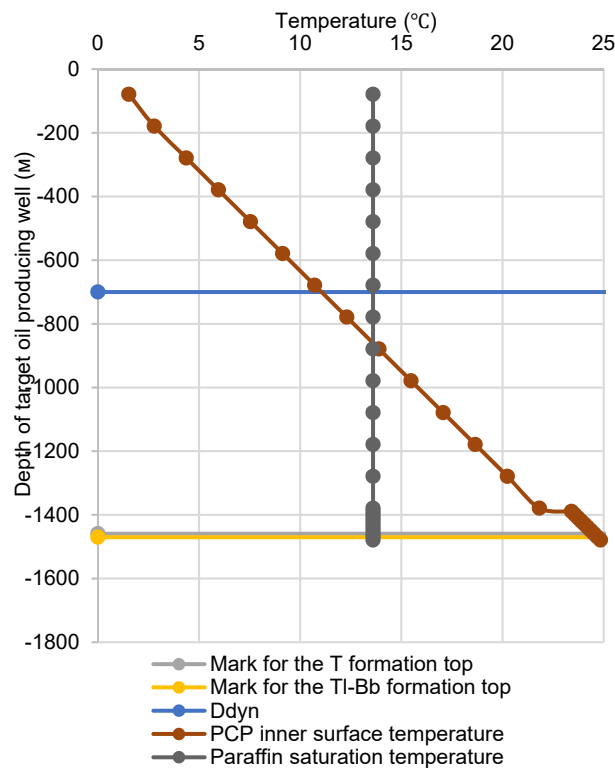


Figure 2. The results of calculating the depth of the starting formation of the organic deposits according to the first group of methods

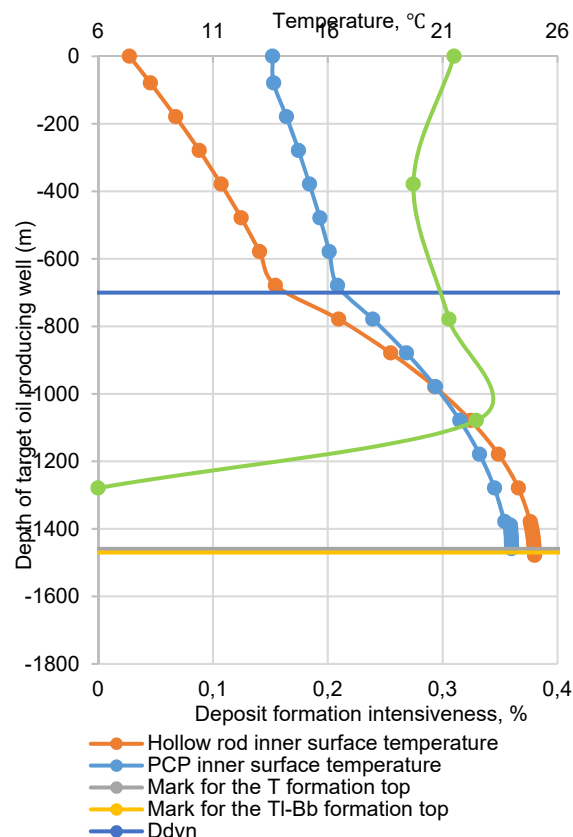


Figure 4. The dependency of the AD formation intensiveness along the hollow rod string

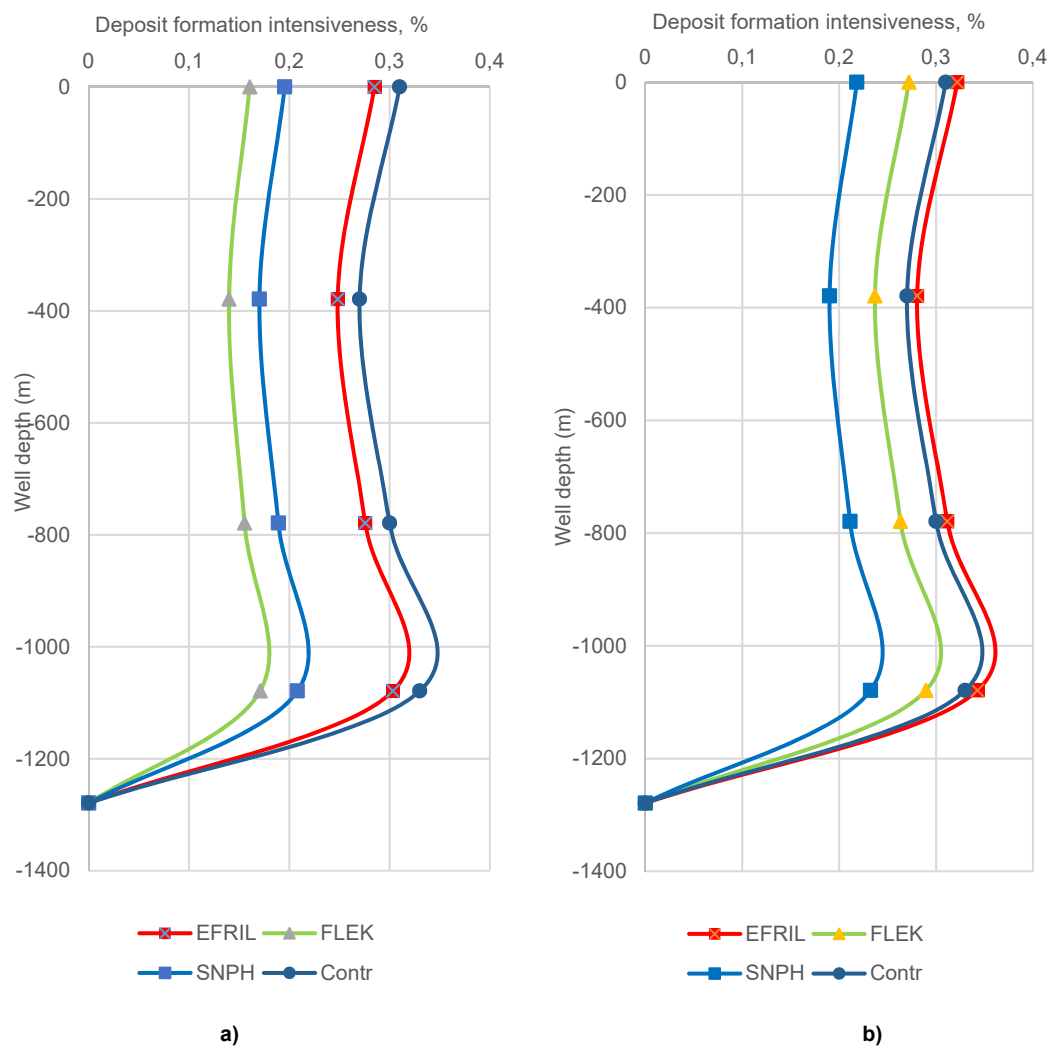


Figure 5. Changes of the AD formation intensiveness in the selected sections: a) upon application of the given inhibitor dose of 200 g/tonne; b) upon application of the given inhibitor dose of 400 g/tonne